

7-3 Super-Conductive Submillimeter-Wave Limb Emission Sounder Onboard International Space Station II: Algorithm Development of for the Data Processing

KASAI Yasuko and OCHIAI Satoshi

We have developed the Superconducting Submillimeter-Wave Limb Emission Sounder (SMILES) planned to onboard International Space Station (ISS) from 1998 in NICT on the collaboration with JAXA. The purpose of the JEM/SMILES instrument is “super sensitive observation” of the minor constituent in the Earth’s atmosphere, such as ClOx, HOx, water vapor and ice cloud. We described the algorithm development to obtain the molecular abundance in the atmosphere from the SMILES spectrum and its data simulation system.

Keywords

Submillimeter-wave, SMILES, International Space Station, Minor constituents, Pollution, atmospheric chemistry

1 Introduction

The Applied Electromagnetic Research Center at NICT has been developing the Superconducting Submillimeter-Wave Limb Emission Sounder (SMILES) for installation aboard the International Space Station (ISS), in collaboration with JAXA, since 1998. SMILES will be mounted on the Japanese Experimental Module (JEM) in the exposed facility of the ISS in 2009. JEM/SMILES consists of a sensor designed for observation of the minor constituents of the Earth’s atmosphere. The sensor receives thermal radiation from substances in the Earth’s atmosphere at high sensitivity, including chlorine- and hydrogen-related man-made air pollutants, water vapor, and ice clouds; the device then performs spectroscopy using the received data.

The key to the high sensitivity of the device lies in the incorporation into JEM/SMILES

of a 4-K-class mechanical freezer and a superconductor receiver (“SIS,” or superconductor-insulator-superconductor, mixer). The frequency range used corresponds to the submillimeter range, consisting of three observation frequency bands (Band A: 624.3 GHz to 625.5 GHz; Band B: 625.1 GHz to 626.3 GHz; and Band C: 649.1 GHz to 650.3 GHz). The observation altitude is from 10 km to 60 km with an anticipated resolution of 3 km to 5 km. The observed area ranges approximately from latitude 65 °N to 38 °S, including areas from the mid-latitudes to the arctic region.

For details of JEM/SMILES, additional documents are available, such as the article “Development of Superconducting Submillimeter-Wave Limb Emission Sounder, SMILES and its Ground Tests” (S. Ochiai, et al.), in Review of the Journal of the National Institute of Information and Communications Technology: Special Issue on Middle and

Upper Atmosphere Observation Technology (Vol.54 Nos.1/2). Here, we discuss the development of the data-analysis algorithm for spectroscopic observation by a millimeter- and submillimeter-wave limb emission sounder such as SMILES, followed by a discussion of the SMILES data-processing simulator.

The SMILES simulator was developed for three purposes: (1) to perform experiments on sensitivity to assist in the development of the data-processing algorithm, (2) to perform error analysis and develop the optimum algorithm within the limit of the determined observation sensitivity of SMILES, and (3) to investigate the development of the basic design of the data-processing system, an aim that NICT has also pursued using the JEM/SMILES simulator.

2 Data-analysis algorithm and calculation method with SMILES simulator: spectral inversion analysis

— Maximum A Posteriori Probability (MAP) Solution —

Here we briefly describe an algorithm for deriving the temperature and the abundance of atmospheric substances from observed SMILES spectra. If the Earth's atmospheric pressure and temperature are constant throughout an observed line of sight, we can determine the abundance of molecules in the line-of-sight column from obtained spectra using the Lambert-Beer Law. However, the pressure and temperature of the real atmosphere vary by altitude. Moreover, we are not seeking to determine the abundance of molecules in a total column but rather the abundance of molecules at each altitude (in other words, to determine the altitude distribution of molecules).

Mathematically, calculating spectra from an altitude distribution of molecules represents a direct problem, while calculating the altitude distribution of molecules from observed spectra is an inverse problem. The operation involved in obtaining an abundance distribu-

tion from spectra is mathematically ill-posed, and we cannot obtain a stable solution. In addition, the solution obtained is not unique. To address these problems, remote sensing observation based on atmospheric spectroscopy generally employs spectral inversion analysis based on Maximum A Posteriori Probability (MAP) to estimate the abundance of molecules at each altitude region of the atmosphere. In millimeter- and submillimeter-wave spectroscopic observation, spectroscopic analysis is usually performed using the Rodgers optimization method, out of a number of available MAP analysis methods. These methods consist of a forward model component, which simulates the observed spectrum and calculates the weighting functions; and a retrieval component, in which spectral inversion analysis is performed. To address the non-linear problem, SMILES also employs the Levenberg-Marquardt iteration scheme.

2.1 Forward model I: Atmospheric radiative transfer equation

The transfer of the radiation emitted from minor molecules in the atmosphere is expressed as indicated below[1].

• Absorption coefficient

The absorption coefficient, α_a , of the molecule "a" can be expressed as follows.

$$\alpha_a = \sum_j \nu I_{saj} e^{E_{aj} \left(1 - \frac{300}{T}\right)} \left(1 - e^{-\frac{(-\Delta E_{aj})}{T}}\right) f \quad (1)$$

Here, j indicates the molecular transition, ν is the frequency, T is the temperature, I_{saj} is the transition intensity, E_{aj} is the ground state energy, and ΔE_{aj} is the energy difference between the states. SMILES mainly uses the JPL catalogue values for these spectroscopic parameters.

In the above equation, f is the linear approximation function[2]. This function is calculated by dividing the altitude into three regions, as follows. Primarily, the Lorentzian profile is used for the low-altitude region, the Gaussian profile is used for the high-altitude

region, and the Voigt profile is used for the intermediate-altitude region. The profiles are selected according to the ratio of the Doppler coefficient, $(x) v_D$, and the Lorentzian coefficient, Δv . Roughly, the ranges are determined as below.

$\Delta v / (x) v_D > 2.0$:	Lorentzian profile
$(x) v / (x) v_D < 0.01$:	Gaussian profile
Other than above:	Voigt profile

The linear approximation function for each profile is expressed by the functions indicated below with line center frequency ν_0 [Hz], temperature T [K], and pressure P [Pa].

Lorentzian profile:

$$f_p = \frac{\Delta v}{\pi \{(\nu - \nu_0)^2 + \Delta v^2\}} \quad (2)$$

$$\Delta v = \Delta v_0 P \left(\frac{296}{T} \right)^n$$

Here, Δv_0 is approximately 2 MHz/hPa to 3 MHz/hPa and n is approximately 0.62 to 0.85.

Gaussian profile:

$$f_D = \frac{\sqrt{\ln 2/\pi} \exp[-\ln 2 \{(\nu - \nu_0)/\Delta v_d\}^2]}{\Delta v_d} \quad (3)$$

$$\Delta v_d = \frac{\nu_0}{c} \sqrt{\frac{2kT \ln 2}{m}}$$

Here, k is the Boltzmann constant, c is the speed of light, and m is the mass of the molecule.

With the Lorentzian profile f_p , and the Gaussian profile f_D , the Voigt profile is expressed as below.

Voigt profile:

$$f_v = \int_{-\infty}^{\infty} f_D(\nu - \nu') f_p(\nu') d\nu' \quad (4)$$

• Continuum absorption by atmosphere and atmospheric water vapor

The continuum absorption by the atmosphere and the atmospheric water vapor is present in the submillimeter range. SMILES uses

the Liebe MPM[3] (millimeter-wave propagation model).

• Attenuation coefficient

Ultimately, the attenuation coefficient, $k\nu$, is the sum of the absorption coefficient obtained for each molecule and the atmospheric continuum absorption by Liebe MPM.

$$k_\nu = \sum_i \alpha_i \frac{x_i P}{kT} + k_{air} \quad (5)$$

Here, k_{air} is the term corresponding to the atmospheric continuum absorption.

• Derivation of brightness temperature for pencil beam

Using the absorption coefficient, a_a , in the previous section, the radiative transfer equation, $T_{\delta\nu}$, for a pencil beam can be expressed as follows.

$$T_{\delta\nu}(s_{near}) = T_{\delta\nu}(s_{far}) \exp\left\{-\int_{s_{far}}^{s_{near}} k_\nu(s) ds\right\} + \int_{s_{far}}^{s_{near}} k_\nu(s) T_e(s) \exp\left\{-\int_s^{s_{near}} k_\nu(s) ds\right\} ds \quad (6)$$

Here, $k\nu$ is the attenuation coefficient discussed above and can be expressed as follows.

$$k_\nu(s_i) = \sum_a \frac{x_a(s_i) P(s_i)}{kT(s_i)} \alpha_\nu^a(s_i) + k_{air}(s_i) \quad (7)$$

Here, s is the variable of the path integral, and s_{far} and s_{near} are the farthest and nearest points from the atmospheric antenna, respectively. x_i is the concentration of the molecule i , τ is the optical thickness, and T_e is the brightness temperature corresponding to the power of black body radiation when the Reyleigh approximation is extended. The latter two quantities are expressed as follows.

$$\tau = \int_s^{s_{near}} \sum_{ij} \alpha_{ij} \frac{x_i P}{kT} ds', \quad (8)$$

$$T_e = \frac{h\nu/k}{e^{h\nu/kT} - 1}$$

Here, h is Planck's constant, and the indices i and j correspond to the molecule and transition quantum number, respectively.

• **Rapid calculation of brightness temperature for pencil beam**

Attempting to calculate the integral of Equation (6) as-is would require an impractically enormous amount of time. Thus, we modify Equation (6) in the form of a recurrence equation, as follows.

$$T_{\delta v}(s_{i+1}) = T_{\delta v}(s_i)\eta_v(s_i, s_{i+1}) + \bar{T}_e(s_i)[1 - \eta_v(s_i, s_{i+1})] \quad (9)$$

Here, $\eta_v(s_i, s_{i+1})$ and $\bar{T}_e(s_i)$ are defined as averages in an interval, as follows.

$$\eta_v(s_i, s_{i+1}) = \exp\left[-\Delta s_i \frac{k_v(s_i) + k_v(s_{i+1})}{2}\right] \quad (10)$$

$$\bar{T}_e(s_i) = \frac{T_e(s_i) + T_e(s_{i+1})}{2}$$

As shown in Fig. 1, Equation (9) is calculated sequentially from the farthest point (s_{far}) from the antenna to the nearest point (s_{near}) to the antenna.

When we use the path indicated in Fig. 1 (i.e., when the path does not cross the Earth), we should use the cosmic background radiation, 3 [K], as the initial value. However, this value can be considered sufficiently close to 0 [K] in the submillimeter frequency range, so we apply 0 [K] to the calculation in the present situation.

• **Step**

Our calculation assumes the steps, Δs_i , in the direction of the limb to be constant. This is because treating Δs_i as constant, as shown in Fig. 2, renders the steps in the direction of altitude fine near the tangent height, which is the most important altitude following conversion to the observed altitude, yielding the ideal conditions for calculation in the direction of the limb.

• **Antenna integration**

As the signal is received by the antenna,

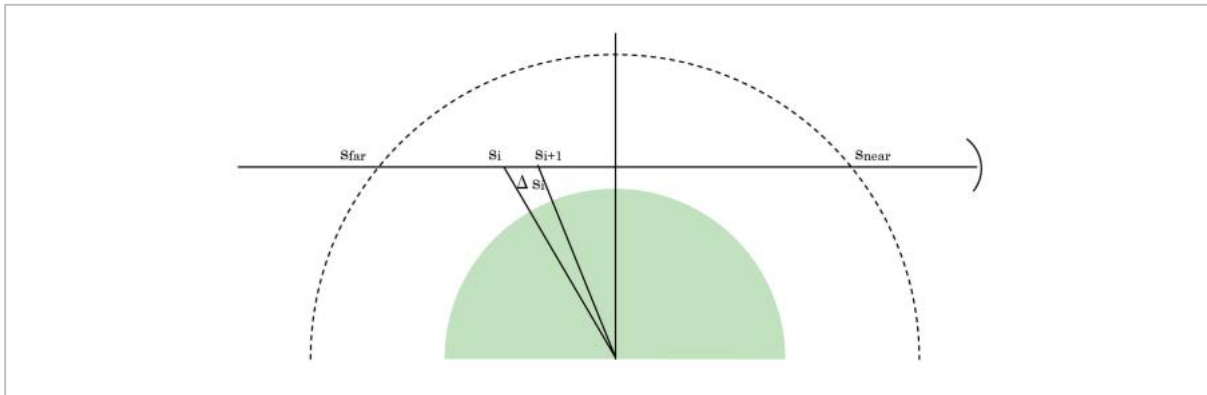


Fig.1 Path (not considering refraction)

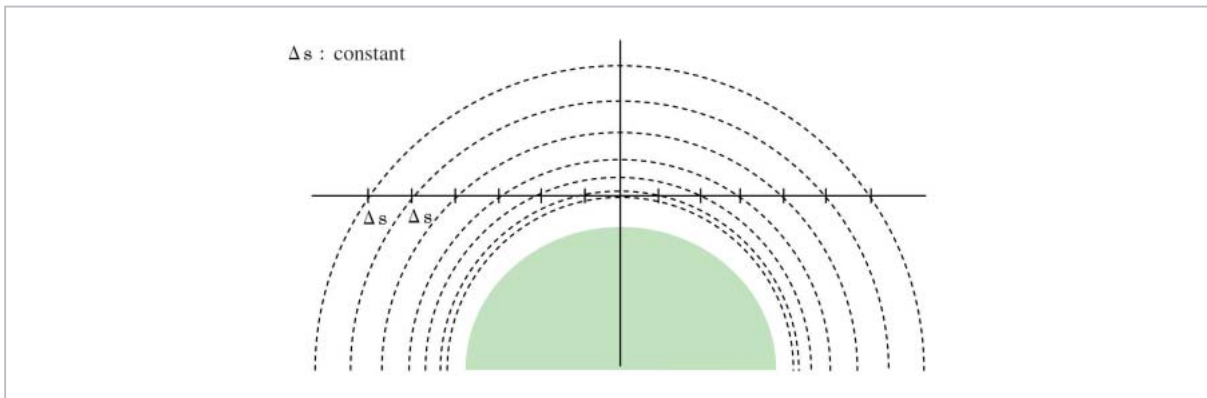


Fig.2 Relationship between steps in direction of limb and steps in direction of altitude

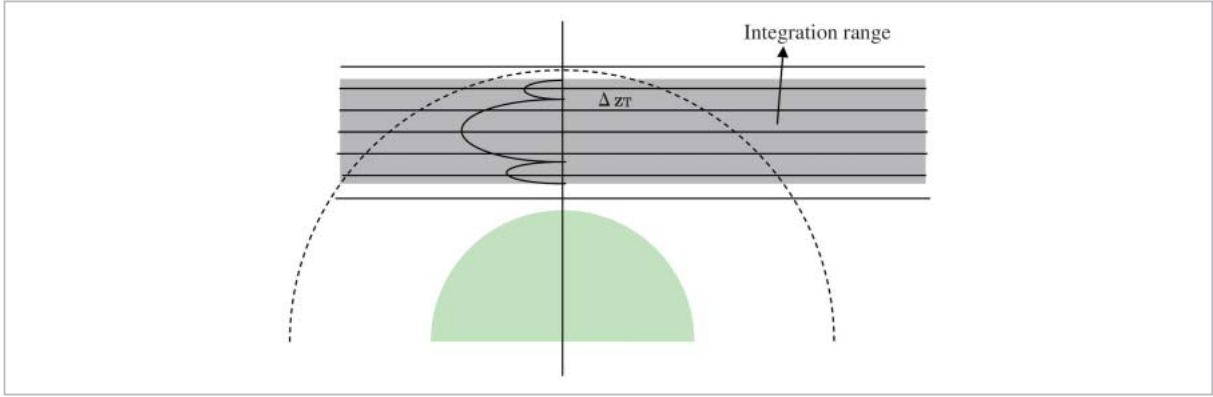


Fig.3 Antenna integration

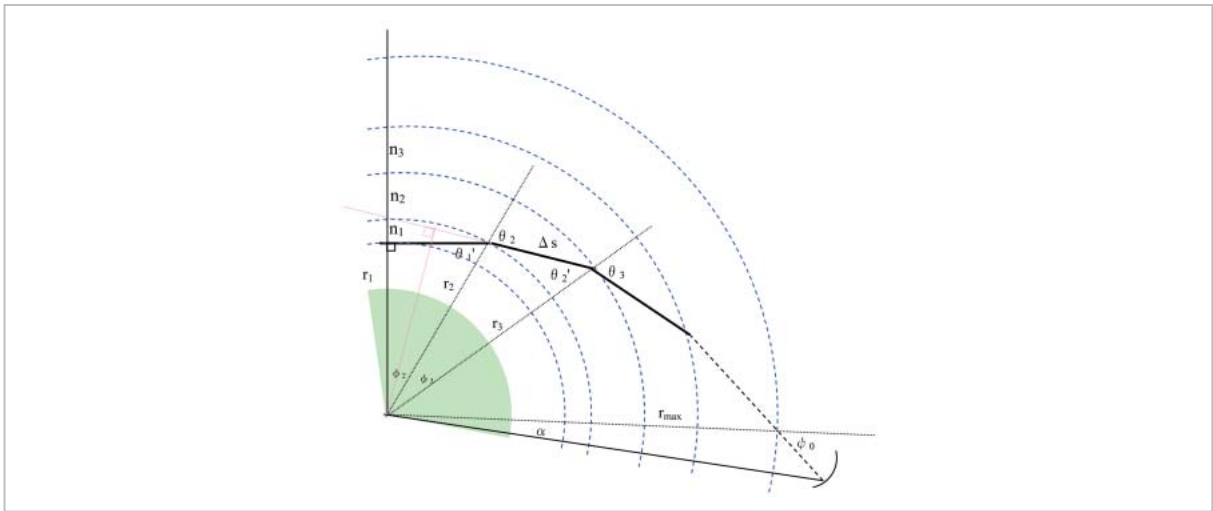


Fig.4 Path taking refraction into consideration (not targeting Earth)

the pencil beam is integrated by antenna width. We now denote the antenna temperature as T_A and the weighting function (which accounts for antenna directionality in the direction of the elevation angle) in the direction of altitude as G . Then, T_A is expressed as follows.

$$T_A = \int_{z_l}^{z_u} G(z_0, z_T) \cdot T_\delta(z_T) dz_T \quad (11)$$

Here, z_u and z_l are the upper and lower limits of the antenna beam. G is normalized and is obtained by projecting the measured values of the antenna profile to each tangent height. The effects of refraction are also taken into consideration.

• Refraction

The millimeter and submillimeter emission transferred through the atmosphere does

not propagate in a straight line but instead undergoes refraction. Particularly in observation in low altitudes where the pressure is high, the effects of refraction are significant. Here, we describe the calculation of the path calculation taking refraction into consideration.

According to Snell's Law, the relationship below holds.

$$n_3 \sin \theta_3 = n_2 \sin \theta_2' \quad (12)$$

From a geometrical point of view, the relationship below holds.

$$r_2 \sin \theta_2 = r_3 \sin \theta_2' \quad (13)$$

From Equations (12) and (13), the relationship below holds.

⟨How to calculate orbit⟩

i	r_i	n_i	θ_i	ϕ_i
1	$z_T + R_e$	$n(z_T)$	90°	—
2	$\sqrt{r_1^2 + \Delta s^2}$	$n(r_2 - R_e)$	$\sin^{-1}\left(\frac{r_1 n_1}{r_2 n_2}\right)$	$\tan^{-1}\left(\frac{\Delta s}{r_1}\right)$
3	$r_2 + \Delta s \sqrt{1 - \left(\frac{r_1 n_1}{r_2 n_2}\right)^2}$	$n(r_3 - R_e)$	$\sin^{-1}\left(\frac{r_1 n_1}{r_3 n_3}\right)$	$\sin^{-1}\left(\frac{\Delta s r_1 n_1}{r_3 r_2 n_2}\right)$
⋮				
i	$r_{i-1} + \Delta s \sqrt{1 - \left(\frac{r_1 n_1}{r_{i-1} n_{i-1}}\right)^2}$	$n(r_i - R_e)$	$\sin^{-1}\left(\frac{r_1 n_1}{r_i n_i}\right)$	$\sin^{-1}\left(\frac{\Delta s r_1 n_1}{r_i r_{i-1} n_{i-1}}\right)$
⋮	Continue to obtain $r_i > r_{\max}$			

$$r_{\max} \cdot 1 \cdot \sin \psi_0 = \dots = r_i n_i \sin \theta_i = \dots = r_3 n_3 \sin \theta_3 = r_2 n_2 \sin \theta_2 = \text{cons.}$$

Next, to obtain the value of this *cons.*, we consider the case in which $\theta_i = 90^\circ$; in other words, at tangent height (z_T). Then, *cons.* is expressed as follows.

$$\text{cons.} = r_1 n_1 = (R_e + z_T) n(z_T)$$

$$\text{Thus, we obtain } \sin \theta_i = \frac{r_1 n_1}{r_i n_i}.$$

We also assume that the following approximate expression holds.

$$r_{i+1} - r_i \approx \Delta s \cos \theta_i$$

The orbit is symmetrical on both sides of the tangent point, as the Earth is assumed to be a perfect sphere.

Finally, we have the following equations.

$$\begin{aligned} \psi_0 &= \sin^{-1} \frac{r_1 n_1}{r_{\max}} \\ \alpha &= \psi_0 - \sin^{-1} \frac{r_{\max} \sin \psi_0}{r_{ISS}} \\ &= \sin^{-1} \frac{r_1 n_1}{r_{\max}} - \sin^{-1} \frac{r_1 n_1}{r_{ISS}} \end{aligned}$$

Thus, the angle from ISS to the tangent point

is given by the following expression.

$$\alpha + \sum_{i=2}^{i_{\max}} \phi_i$$

This expression is used for determining the range when we consider inhomogeneity in the horizontal direction.

Here we use the following expression for refraction, $n(z)$.

$$n(z) = 315 \exp(-z/7.35) \times 10^{-6} + 1$$

2.2 Forward model II : Instrumental function

In Forward model II, we apply the instrumental function to the radiation received by the antenna and produce the spectrum derived from the observation[4].

• Overview of SMILES system

Figure 5 shows a schematic diagram of the SMILES system.

The flow of the instrumental function calculation is indicated below.

Flow of SMILES instrumental calculation.

Due to the limited space of this article, here we only describe the calculation related to the AOS spectrometer among the components of the system.

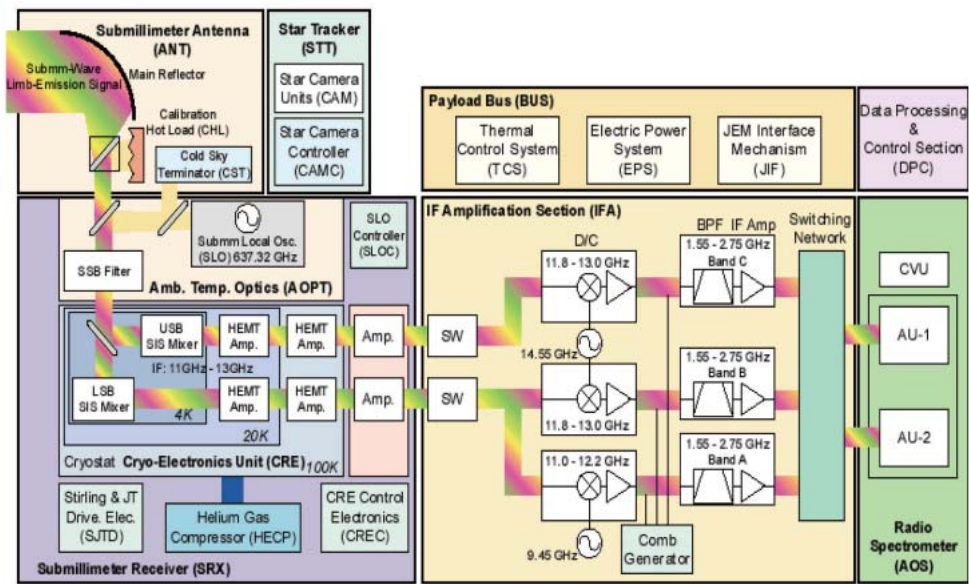


Fig.5 SMILES system (reproduced from SMILES Mission Plan)

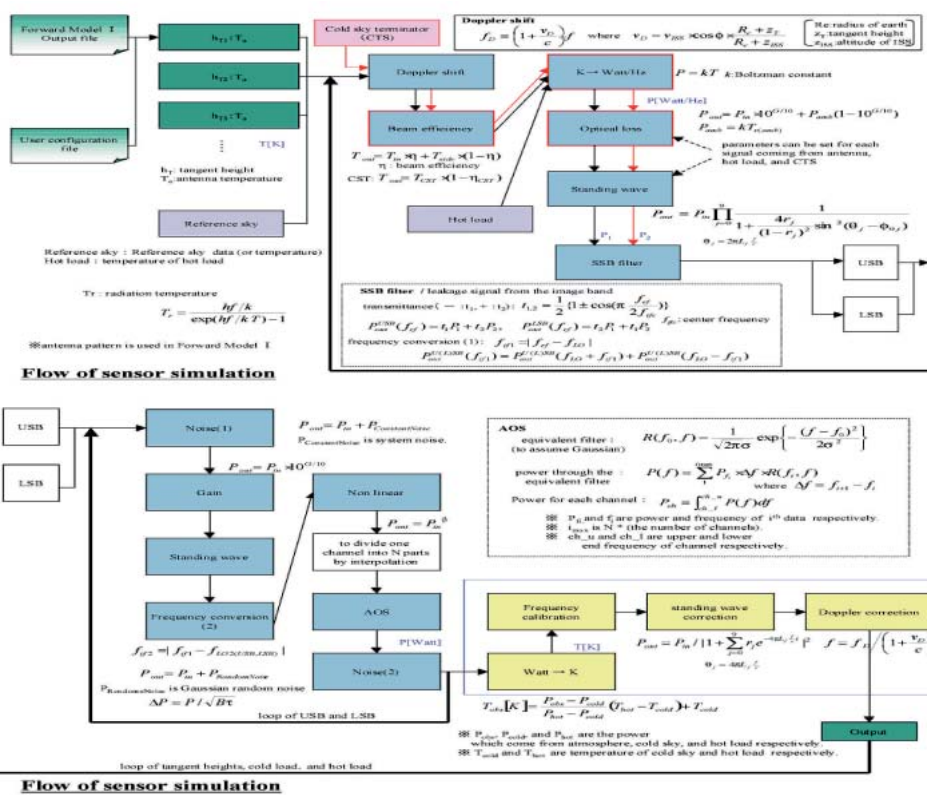


Fig.6 Flow of instrumental calculation

- **AOS (Acousto-Optic Spectrometer)**
 SMILES uses the AOS spectrometer.
 First, the signal from the antenna goes

through the transducer and propagates as a sound wave (i.e., a compressional wave) in the crystal. When the light (at 780 nm) from a laser diode is irradiated to the crystal, the light

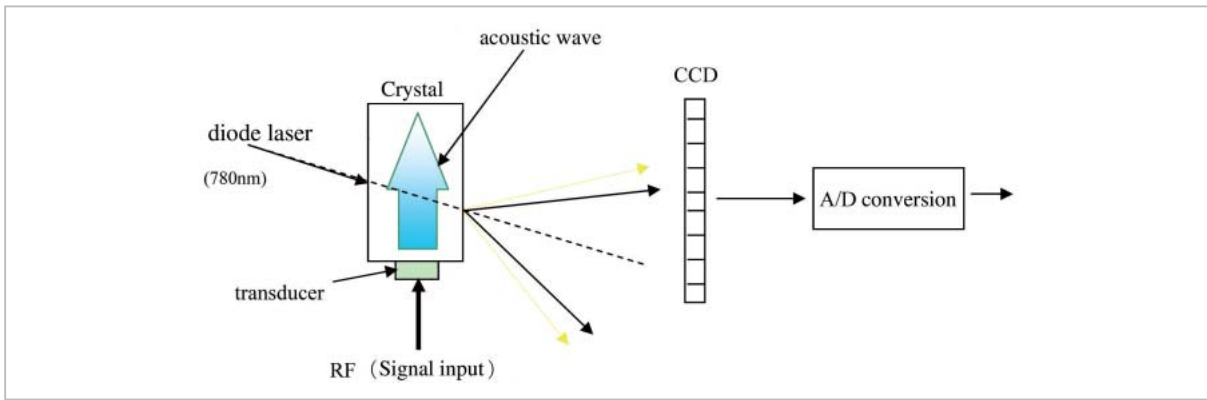


Fig.7 AOS

undergoes Bragg diffraction. A CCD camera captures the first-order diffracted light. Here, if the input signal contains two or more frequency components, they are diffracted in different directions, and the directions of the first order diffracted light vary accordingly. Thus, the signals enter different CCD cameras,

enabling us to separate the frequency components in the input signal in this manner.

However, AOS has a characteristic channel response and outputs a broader signal even if a single frequency signal is input. We now move on in our discussion to the handling of this effect in the simulator.

○ **When the input signal is a single frequency signal**

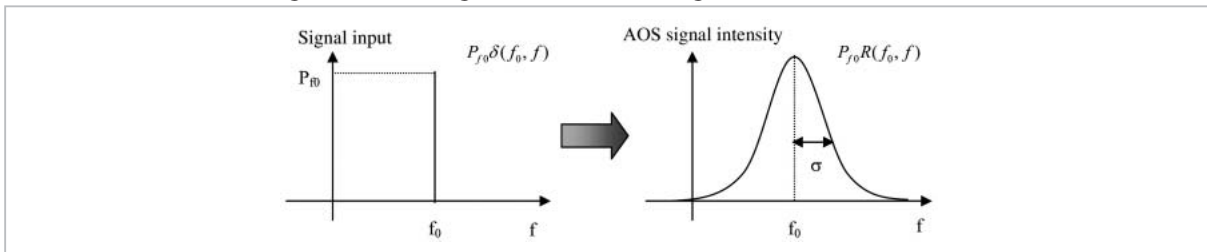


Fig.8 Channel response function

Here, δ takes values as follows.

$$\delta = \begin{cases} 1 & f = f_0 \\ 0 & f \neq f_0 \end{cases} \quad (14)$$

R is a normalized function.

(Example) For Gaussian

$$R(f) = \frac{1}{\sqrt{2\pi}\sigma} \exp\left\{-\frac{(f-f_0)^2}{2\sigma^2}\right\} \quad (15)$$

○ **When the input frequency is continuous**

$P(f')\delta(f', f) \rightarrow$ (discretely expressed)

$$\rightarrow \sum_{i_{\min}}^{i_{\max}} P_{f_i} \delta(f_i, f)$$

↓ Through AOS

$$\sum_{i_{\min}}^{i_{\max}} P_{f_i} R(f_i, f)$$

Next, we describe the simulator's handling of operation at the output of the CCD camera. There are 1,500 CCD cameras installed for a single AOS. The frequency range of a single channel of an CCD camera corresponds to 0.8 MHz. Thus, we integrate the data in a channel width of 0.8 MHz.

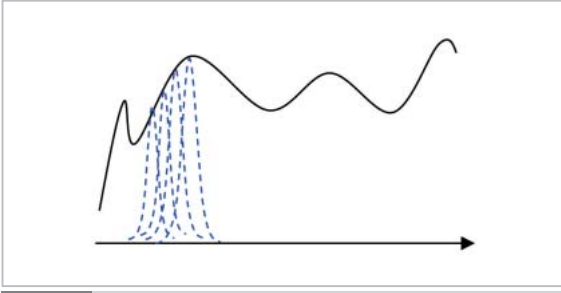


Fig.9 When input frequency is continuous

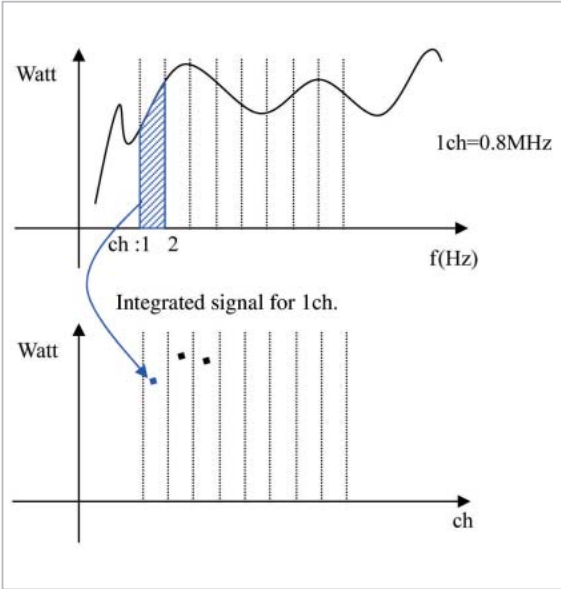


Fig.10 Conversion to data per channel

2.3 Forward model III: Weighting functions (WF)

• WF for deriving atmospheric molecules

The brightness temperature is calculated as follows.

$$T_{\delta v}(s_{i+1}) = T_{\delta v}(s_i)\eta_v(s_i, s_{i+1}) + \bar{T}_e(s_i)[1 - \eta_v(s_i, s_{i+1})] \quad (16)$$

$$\eta_v(s_i, s_{i+1}) = \exp\left[-\Delta s_i \frac{k_v(s_i) + k_v(s_{i+1})}{2}\right] \quad (17)$$

$$\bar{T}_e(s_i) = \frac{T_e(s_i) + T_e(s_{i+1})}{2}$$

The WF for the line of sight (LOS) can be defined as follows.

$$K_{HT}(v, s_i) = \frac{\partial T_v(s_N)}{\partial k_v(s_i)} \cdot \frac{\partial k_v(s_i)}{\partial x_a(s_i)} \quad (18)$$

The factors in the equation are expressed as

follows.

$$\frac{\partial k_v(s_i)}{\partial x_a(s_i)} = \frac{P(s_i)}{kT(s_i)} \alpha_v^a(s_i) \quad (19)$$

$$\frac{\partial T_v(s_N)}{\partial k_v(s_0)} = -\frac{\Delta s}{2} [T_v(s_0) - \bar{T}_e(s_0)] \eta(s_0, s_N)$$

$$\frac{\partial T_v(s_N)}{\partial k_v(s_i)} = -\frac{\Delta s}{2} [2(T_v(s_{i-1}) - \bar{T}_e(s_{i-1}))\eta(s_{i-1}, s_i) + T_v(s_i) - \bar{T}_e(s_{i-1}))\eta(s_i, s_N)] \quad (20)$$

$$\frac{\partial T_v(s_N)}{\partial k_v(s_N)} = -\frac{\Delta s}{2} [T_v(s_{N-1}) - \bar{T}_e(s_{N-1})] \eta(s_{N-1}, s_N)$$

Here, the following expression is used.

$$\eta(s_i, s_N) = \eta(s_i, s_{i+1})\eta(s_{i+1}, s_{i+2}) \cdots \eta(s_{N-1}, s_N) \quad (21)$$

Next, we convert this WF for the LOS to the WF for the altitude.

The WF in the direction of the altitude is expressed as follows.

$$K_{HT}(v, z_i) = \sum_j \frac{\partial T_v(s_N)}{\partial k_v(s_j)} \cdot \frac{\partial k_v(s_j)}{\partial k_v(z_i)} \cdot \frac{\partial k_v(z_i)}{\partial x_a(z_i)} \quad (22)$$

Here, the following equation is used.

$$\frac{\partial k_v(z_i)}{\partial x_a(z_i)} = \frac{P(z_i)}{kT(z_i)} \alpha_v^a(z_i) \quad (23)$$

$\frac{\partial T_v(s_N)}{\partial k_v(s_j)}$ is the same as in Equation (20).

Thus, if we obtain the middle term, $\frac{\partial k_v(s_i)}{\partial k_v(z_i)}$,

we can obtain the WF for the altitude.

Thus, we use the following expression.

$$k_v(z) = \sum_i k_v(z_i)\phi_i(z) \quad (24)$$

Here, we assume the linear interpolation.

Then, ϕ is expressed as follows.

$$\phi_i(z) = \begin{cases} 0 & (z < z_{i-1}, z_{i+1} < z) \\ \frac{z - z_{i-1}}{z_i - z_{i-1}} & (z_{i-1} < z < z_i) \\ \frac{z_{i+1} - z}{z_{i+1} - z_i} & (z_i < z < z_{i+1}) \end{cases} \quad (25)$$

Then, we obtain the following equation.

$$\frac{\partial k_v(s_i)}{\partial k_v(z_i)} = \phi_i(z) \quad (26)$$

Thus, the WF for the altitude is expressed as in the following equation. (Fig. 12)

$$K_{hT}(v, z_i) = \sum_j \frac{\partial T_v(s_N)}{\partial k_v(s_j)} \cdot \phi_i(z(s_j)) \cdot \frac{\partial k_v(z_i)}{\partial x_a(z_i)} \quad (27)$$

• WF for deriving temperature

The WF for the temperature can be expressed as below with the variable conversion expressed in Equation (23)

$$K_T(v, z_i) \equiv \frac{\partial T_v(s_{near})}{\partial T(z_i)} \quad (28)$$

$$= \sum_j \frac{\partial T_v(s_{near})}{\partial k_v(s_j)} \cdot \frac{\partial k_v(s_j)}{\partial k_v(z_i)} \cdot \frac{\partial k_v(z_i)}{\partial T(z_i)}$$

The first term,

$$\sum_j \frac{\partial T_v(s_{near})}{\partial k_v(s_j)} \cdot \frac{\partial k_v(s_j)}{\partial k_v(z_i)}$$

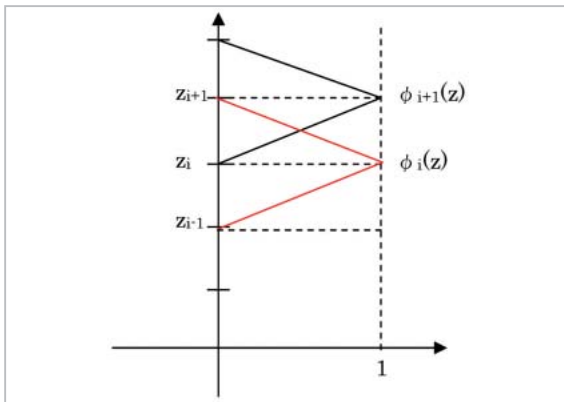


Fig. 11 Definition of f

is the same as in the calculation of the WF for the molecular concentration. In the case of the WF for the temperature, we calculate $\frac{\partial k_v(z_i)}{\partial x(z_i)}$

for each altitude instead of $\frac{\partial k_v(z_i)}{\partial T(z_i)}$ in the calculation of the WF for the molecular concentration.

For Lorentzian:

$$\frac{\partial k_v(z_i)}{\partial T(z_i)} = \sum_a \frac{x_a(z_i)P(z_i)}{kT(z_i)} \sum_{u,l} \left\{ \frac{300[K] \cdot E}{T(z_i)^2} \right. \quad (29)$$

$$\left. + \frac{\Delta E \cdot e^{-\frac{\Delta E}{T}}}{T(z_i)^2 \left(1 - e^{-\frac{\Delta E}{T}}\right)} - \frac{n}{T} (1 - 2\pi f_L \gamma_L) - \frac{1}{T} \right\}$$

$$S_{a,ul}(T(z_i)) \cdot F_a(v, v_{ul})$$

For Gaussian:

$$\frac{\partial k_v(z_i)}{\partial T(z_i)} = \sum_a \frac{P(z_i)}{kT(z_i)} \sum_{u,l} \left\{ \frac{300[K] \cdot E}{T(z_i)^2} + \frac{\Delta E \cdot e^{-\frac{\Delta E}{T}}}{T(z_i)^2 \left(1 - e^{-\frac{\Delta E}{T}}\right)} \right. \quad (30)$$

$$\left. + \left\{ \frac{(v - v_0)^2}{\gamma_D^2 T(z_i)} - \frac{1}{2T(z_i)} \right\} - \frac{1}{T(z_i)} \right\} \cdot S_{a,ul}(T(z_i))$$

$$\cdot F_a(v, v_{ul})$$

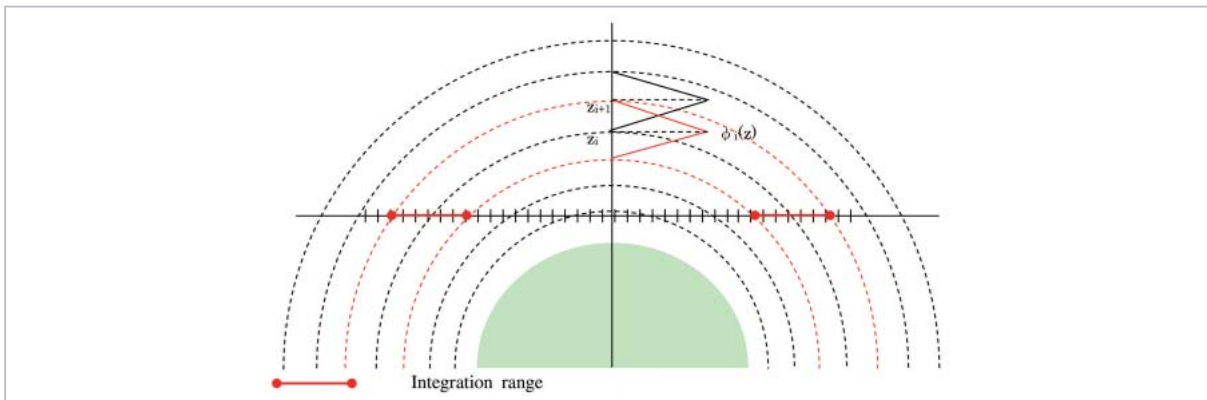


Fig. 12 Calculation of WF in direction of altitude

2.4 Inversion analysis

Here, we briefly describe the Rodgers optimization method[5]-[7].

The observed value, \mathbf{y} , can be expressed as follows.

$$\mathbf{y} = \mathbf{F}(\mathbf{x}) + \boldsymbol{\varepsilon} \quad (31)$$

Here, \mathbf{y} is the observed vector and \mathbf{x} is an unknown vector such as the altitude distribution of the molecular abundance, $\boldsymbol{\varepsilon}$ is the vector of the observed errors, and \mathbf{F} is the forward model.

When we express Equation (31) with a linear approximation using a priori \mathbf{x}_a , we obtain the following expression.

$$\begin{aligned} \mathbf{y} &= \frac{\partial \mathbf{F}}{\partial \mathbf{x}} (\mathbf{x} - \mathbf{x}_a) + \boldsymbol{\varepsilon} \\ &= \mathbf{K} \cdot (\mathbf{x} - \mathbf{x}_a) + \boldsymbol{\varepsilon} \end{aligned} \quad (32)$$

Here, \mathbf{K} is the weighting function (WF) for the concentration, temperature, or other quantities. The components of the vectors are explicitly expressed as follows.

$$\mathbf{y} = \begin{pmatrix} y_{11} \\ y_{12} \\ y_{13} \\ y_{21} \\ y_{22} \\ y_{23} \\ y_{31} \\ \vdots \end{pmatrix},$$

$$\mathbf{K} = \begin{pmatrix} K_{11}^1(z_1) K_{11}^1(z_2) & K_{11}^2(z_1) K_{11}^2(z_2) & K_{b11}^1 \\ K_{12}^1(z_1) K_{12}^1(z_2) & K_{12}^2(z_1) K_{12}^2(z_2) & K_{b12}^1 \\ K_{13}^1(z_1) K_{13}^1(z_2) & \dots & K_{b13}^1 \\ K_{21}^1(z_1) K_{21}^1(z_2) & K_{21}^2(z_1) K_{21}^2(z_2) & \dots & K_{b21}^1 \\ K_{22}^1(z_1) K_{22}^1(z_2) & K_{22}^2(z_1) K_{22}^2(z_2) & & K_{b22}^1 \\ \vdots & \vdots & \vdots & \vdots & \vdots \end{pmatrix},$$

$$\mathbf{x} = \begin{pmatrix} x^1(z_1) \\ x^1(z_2) \\ \vdots \\ x^2(z_1) \\ \vdots \\ b_1 \\ \vdots \end{pmatrix}, \quad \mathbf{x}_a = \begin{pmatrix} x_a^1(z_1) \\ x_a^1(z_2) \\ \vdots \\ x_a^2(z_1) \\ \vdots \\ b_1 \\ \vdots \end{pmatrix}$$

The indices ij for y_{ij} and K_{ij} correspond to the tangent height h_i and the frequency ν_j , and z_1 ,

z_2, \dots are the steps in the altitude.

The unknown vector ($\hat{\mathbf{x}}$) to be obtained can be expressed as follows.

$$\hat{\mathbf{x}} = \mathbf{x}_a + \mathbf{D} \cdot (\mathbf{y} - \mathbf{y}_a) \quad (33)$$

Here, \mathbf{y}_a is the brightness temperature calculated using the a priori altitude profile, \mathbf{x}_a , \mathbf{K}_a is the weighting function (WF) calculated from \mathbf{x}_a .

\mathbf{D} in Equation (33) is expressed as follows.

$$\mathbf{D} = (\mathbf{K}^T \mathbf{S}_y^{-1} \mathbf{K} + \mathbf{S}_a^{-1})^{-1} \mathbf{K}^T \mathbf{S}_y^{-1} \quad (34)$$

\mathbf{S}_y : Variance-covariance matrix of observed data

\mathbf{S}_a : A priori variance-covariance matrix

Further, if we express as $\mathbf{A} = \mathbf{D} \cdot \mathbf{K}$, we obtain the following expression.

$$\hat{\mathbf{x}} = (\mathbf{I} - \mathbf{A}) \cdot \mathbf{x}_a + \mathbf{A} \cdot \mathbf{x} \quad (35)$$

Here, \mathbf{A} is referred to as the averaging kernel. We can find the resolution of the result of the retrieval in the direction of altitude by observing the components of the averaging kernel in the direction of the row.

The dispersion, \mathbf{S} , of the error in the results of analysis is given by the following equation.

$$\mathbf{S} = (\mathbf{I} - \mathbf{A}) \cdot \mathbf{S}_a \quad (36)$$

4 Conclusions

This article describes the spectral data processing algorithm and simulator used and developed in the JEM/SMILES project. JAXA is now endeavoring to generate a detailed design of the data-processing system, based on the results of this study.

Acknowledgment

We would like to express our sincere gratitude to Ms. Chikako Takahashi of Fujitsu FIP Corporation, who contributed greatly to the development of the simulator, including its coding.

References

- 1 Ochiai, S., MAES, The proceedings of the forward model workshop, Bremen, Apr. 1999.
- 2 M. Kuntz, "A new implementation of the humlicek algorithm for the calculation of the Voigt profile function", JQSRT, Vol.57, No6, pp.819-824, 1997.
- 3 Liebe, H. J. and G. A. Hufford, Modeling millimeter-wave propagation effects in the atmosphere, AGARD CP-454, 18, NATO, 1989.
- 4 T. Manabe, Effects of Atmospheric Refraction on Limb Sounding from JEM/SMILES, available at <http://www.crl.go.jp/ck/ck321/smiles/refrac/refrac.pdf>.
- 5 Rodgers, C. D., "Characterization and error analysis of profiles retrieved from remote sounding measurements", J. Geophys. Res, Vol.95, No.FD5, pp.5587-5595, 1990.
- 6 Rodgers, C. D., "Retrieval of atmospheric temperature and composition from remote measurements of thermal radiation", Rev. Geophysics and space Physics, 14(4), 609-624, 1976.
- 7 Stefan Buhler, Patrick Eriksson, ARTS USER GUIDE, Jun. 17, 2000, ARTS Version 2000.

KASAI Yasuko, Dr. Sci.
*Senior Researcher, Environment
Sensing and Network Group, Applied
Electromagnetic Research Center
Terahertz Remote Sensing*

OCHIAI Satoshi
*Senior Researcher, Environment
Sensing and Network Group, Applied
Electromagnetic Research Center
Microwave Remote Sensing*